LETTER

doi:10.1038/nature11083

A unifying model for mTORC1-mediated regulation of mRNA translation

Carson C. Thoreen[1,2,3], Lynne Chantranupong[3,4,5], Heather R. Keys[3,4,5], Tim Wang[3,4], Nathanael S. Gray[1,2] & David M. Sabatini[3,4,5]

The mTOR complex 1 (mTORC1) kinase nucleates a pathway that promotes cell growth and proliferation and is the target of rapamycin, a drug with many clinical uses[1]. mTORC1 regulates messenger RNA translation, but the overall translational program is poorly defined and no unifying model exists to explain how mTORC1 differentially controls the translation of specific mRNAs. Here we use high-resolution transcriptome-scale ribosome profiling to monitor translation in mouse cells acutely treated with the mTOR inhibitor Torin 1, which, unlike rapamycin, fully inhibits mTORC1 (ref. 2). Our data reveal a surprisingly simple model of the mRNA features and mechanisms that confer mTORC1-dependent translation control. The subset of mRNAs that are specifically regulated by mTORC1 consists almost entirely of transcripts with established 5′ terminal oligopyrimidine (TOP) motifs, or, like *Hsp90ab1* and *Ybx1*, with previously unrecognized TOP or related TOP-like motifs that we identified. We find no evidence to support proposals that mTORC1 preferentially regulates mRNAs with increased 5′ untranslated region length or complexity[3]. mTORC1 phosphorylates a myriad of translational regulators, but how it controls TOP mRNA translation is unknown[4]. Remarkably, loss of just the 4E-BP family of translational repressors, arguably the best characterized mTORC1 substrates, is sufficient to render TOP and TOP-like mRNA translation resistant to Torin 1. The 4E-BPs inhibit translation initiation by interfering with the interaction between the cap-binding protein eIF4E and eIF4G1. Loss of this interaction diminishes the capacity of eIF4E to bind TOP and TOP-like mRNAs much more than other mRNAs, explaining why mTOR inhibition selectively suppresses their translation. Our results clarify the translational program controlled by mTORC1 and identify 4E-BPs and eIF4G1 as its master effectors.

The mTOR kinase is the catalytic subunit of two complexes, mTORC1 and 2, which regulate growth and are often deregulated in disease (reviewed in ref. 1). mTORC1 is the allosteric target of the well-known drug rapamycin, which has clinical uses in organ transplantation, cardiology and oncology. A major function of mTORC1 is to regulate protein synthesis, which it is thought to control through several substrates, including the S6 kinases (S6Ks), the inhibitory eIF4E-binding proteins (4E-BPs), and the eIF4G initiation factors. ATP-competitive inhibitors of mTOR such as Torin 1 impair protein synthesis and proliferation to a much greater degree than rapamycin[1,2], largely owing to their inhibition of rapamycin-resistant functions of mTORC1. Because earlier efforts to identify mRNAs translationally regulated by mTORC1 relied on rapamycin[5–7], it is likely that the mTORC1-regulated translational program is not fully defined.

As a step towards defining this program, we examined the effects of Torin 1 on protein synthesis in mouse embryonic fibroblasts (MEFs). To focus on the direct translational outputs of mTORC1 and avoid secondary effects, we treated cells with Torin 1 for only 2 h. Torin 1 blocked canonical mTORC1-dependent events, such as the phosphorylation of S6K1 and 4E-BP1, but did not increase the phosphorylation of eIF2α, which represses translation and is induced by stresses like amino acid deprivation (Fig. 1a). In wild-type MEFs, Torin 1 suppressed ^{35}S-Cys/Met incorporation into protein by ~65% and shifted ribosomes out of polysomes, indicating that mTOR inhibition causes a severe defect in translation initiation (Fig. 1b, c).

To monitor systematically the translation of individual mRNAs, we analysed vehicle- and Torin-1-treated MEFs using transcriptome-scale ribosome profiling[8]. Ribosome profiling provides a precise measurement of mRNA translation by quantifying ribosome-protected mRNA fragments (ribosome footprints (RFs)) using deep sequencing. In proliferating MEFs, we detected 3.9 million exon-mapped ribosome footprints that corresponded to 12,856 actively translated RefSeq (http://www.ncbi.nlm.nih.gov/RefSeq/) mRNAs. Of these, 4,840 could be monitored at levels sufficient for robust measurements of Torin-1-induced translational changes (Supplementary Table 1). The frequency of RFs that map to each mRNA (gene-specific reads per million total exon-mapped reads, or RPM) reflects the proportion of ribosomes engaged in the translation of that transcript. In vehicle- and Torin-1-treated cells, the distributions of RF frequencies were largely superimposable (median $\log_2$(change in RF frequency) = 0.08), arguing that mTOR inhibition has similar effects on the translation of most mRNAs (Fig. 1d). Given this and the ^{35}S-Cys/Met incorporation results (Fig. 1b), we determined (see Methods) that mTOR inhibition suppresses the translation of nearly all (99.8%) mRNAs to some degree, with a mean reduction in translation of 61% (median = 60.5%). Consistent with this conclusion, β-actin mRNA, which, like most mRNAs, underwent little change in RF frequency upon Torin 1 treatment ($\log_2(\Delta RPM) = -0.08$), was nevertheless partially but significantly depleted from polysomes in Torin-1-treated cells (Fig. 1e). Thus, acute mTOR inhibition has the unappreciated capacity to moderately suppress the translation of nearly all mRNAs.

To identify the mRNAs most regulated by mTOR at the translational level, we calculated the Torin-1-induced change in the translational efficiency of each mRNA (Fig. 1f). This measurement normalizes RF frequency to the abundance of the corresponding transcript and so decouples translational and transcriptional regulation. Using a *z*-score cut-off of ±1.5, we selected 253 suppressed and 198 resistant mRNAs for further analysis. Gene ontology analyses of Torin-1-suppressed mRNAs showed enrichment for those involved in various steps in protein synthesis (Supplementary Fig. 1a), albeit with differences among components of the translational machinery (Fig. 1g and Supplementary Table 2). For instance, Torin 1 suppressed the translation of *Eif4b* but not of other eIF4F complex components, and of nearly all cytoplasmic ribosomal proteins, except *Rps27a*, which has extra-ribosomal functions[9]. Torin-1-resistant mRNAs are enriched for transcription factors (Supplementary Fig. 1a), such as *Stra13*, *Myc*, *Paf1* and *Foxo1*. Additionally, the translation of mRNAs with putative internal ribosomal entry sites (IRES)[10,11] and, unexpectedly, those encoding histones

[1]Department of Cancer Biology, Dana Farber Cancer Institute, 250 Longwood Avenue, Boston, Massachusetts 02115, USA. [2]Department of Biological Chemistry and Molecular Pharmacology, Harvard Medical School, 250 Longwood Avenue, Boston, Massachusetts 02115, USA. [3]Whitehead Institute for Biomedical Research, Nine Cambridge Center, Cambridge, Massachusetts 02142, USA. [4]Howard Hughes Medical Institute and Department of Biology, Massachusetts Institute of Technology, Cambridge, Massachusetts 02139, USA. [5]Broad Institute of Harvard and MIT, Seven Cambridge Center, Cambridge, Massachusetts 02142, USA.

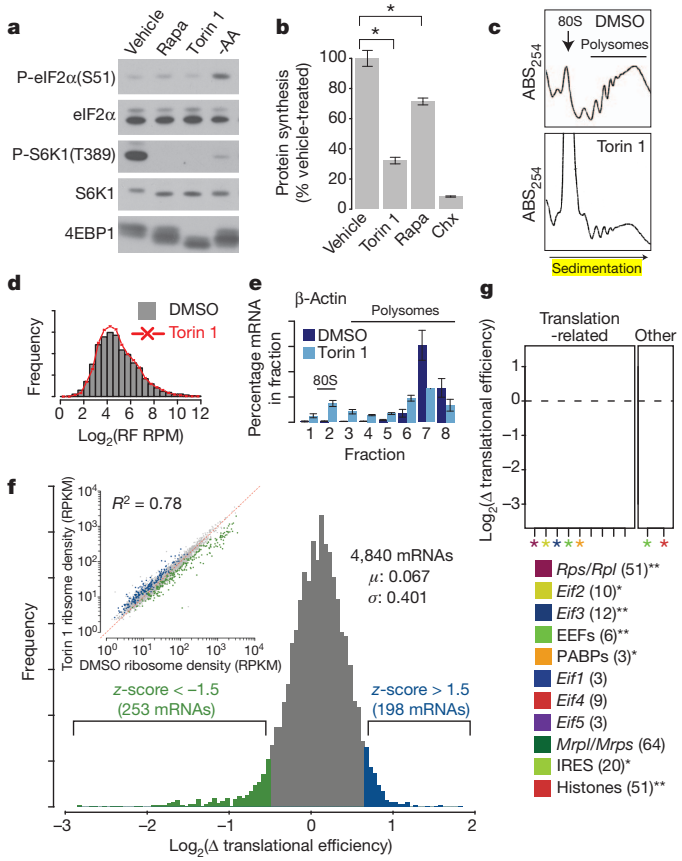

Figure 1 | Profile of mTOR-regulated translation. **a**, Wild-type MEFs were treated with vehicle (DMSO), 250 nM rapamycin (Rapa) or Torin 1, or starved for amino acids (−AA) for 2 h and analysed for protein levels. P, phospho. **b**, Wild-type MEFs were treated for 2 h with vehicle (DMSO), 250 nM rapamycin or Torin 1, or 10 μg ml^{-1} cycloheximide (Chx), pulsed for 30 min with ^{35}S-Cys/Met and ^{35}S incorporation into protein quantified and normalized to the total protein. Data are mean ± s.d. ($n = 3$). *$P < 0.005$. **c**, Polysome profiles of wild-type MEFs treated with DMSO or 250 nM Torin 1 for 2 h. ABS_{254}, absorbance of light at 254 nm. **d**, Distributions of RF frequency in vehicle- or Torin-1-treated cells. RF libraries from cells treated as in **c** were used to determine RF frequencies (RPM) for 4,840 mRNAs. **e**, β-Actin mRNA abundance in fractions from **c** were quantified by quantitative polymerase chain reaction (qPCR), and calculated as a percentage of the total in all fractions. Data are means ± s.e.m. ($n = 2$). **f**, Distribution of changes in translational efficiency from vehicle- or Torin-1-treated cells. RF frequencies from **d** were normalized to transcript levels to calculate translational efficiencies. Ribosome densities (reads per kilobase per million, RPKM) from vehicle- and Torin-1-treated cells are inset. mRNAs with suppressed (z-score < −1.5) or resistant (z-score > 1.5) translational efficiencies are indicated. **g**, Torin-1-dependent changes in translational efficiency for indicated mRNA classes. For histone mRNAs, results reflect changes in ribosome density only. Significance determined by two-tailed Mann–Whitney U test. *$P < 0.005$, **$P < 0.0005$.

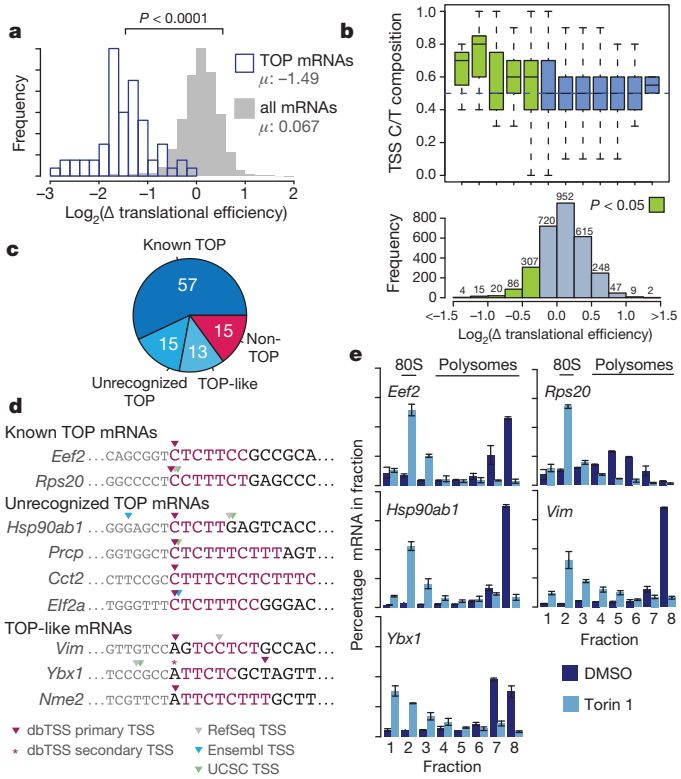

Figure 2 | Translation of TOP and TOP-like mRNAs is hypersensitive to mTOR inhibition. **a**, Torin-1-induced changes in translational efficiencies of 65 known TOP mRNAs in wild-type MEFs (outlined bars) compared to changes in all 4,840 mRNAs (solid bars). Significance determined by the Mann–Whitney U test. **b**, The pyrimidine content of the 10 nucleotides surrounding the TSS for 3,025 mRNAs where the TSS could be confidently identified, excluding 65 known TOP mRNAs (expected frequency = 0.518). Box plots indicate the TSS pyrimidine content for mRNAs binned according to Torin-1-dependent change in translational efficiency. Significance determined by binomial test. **c**, Numbers of indicated mRNA classes. **d**, TSS annotations for selected TOP and TOP-like mRNAs. Primary and secondary TSS locations from dbTSS (purple) are indicated, as are annotations from RefSeq (grey), Ensembl (blue), and UCSC (green). **e**, Polysome analyses of selected TOP (*Eef2*, *Rps20*), unrecognized TOP (*Hsp90ab1*) and TOP-like (*Vim*, *Ybx1*) mRNAs. Data are means ± s.e.m. ($n = 2$).

were also clearly resistant to Torin 1 (Fig. 1g), indicating that these mRNAs use modes of initiation that do not depend on mTOR activity[12].

We considered the features that define the mRNAs that are most translationally suppressed upon mTOR inhibition. Two types of mRNAs are thought to be highly mTOR-dependent: (1) those with long and complex 5′ untranslated regions (UTRs) that are reported to be regulated through a 4E-BP-dependent mechanism[3]; and (2) mRNAs with 5′ TOP motifs that are regulated through an unknown mechanism[13]. Surprisingly, the translational efficiency of commonly cited examples of mRNAs with long, complex UTRs, such as cyclin D1 ($\log_2(\Delta) = -0.07$), cyclin D3 ($\log_2(\Delta) = 0.09$), *Myc* ($\log_2(\Delta) = 0.92$) and *Vegfa* ($\log_2(\Delta) = 0.79$)[14], was not significantly suppressed in our data set. We found no evidence that 5′ UTR length or complexity correlated positively with sensitivity to mTOR inhibition and, if anything, mRNAs with shorter and less complex 5′ and 3′ UTRs tended to be more sensitive (Supplementary Fig. 1b–d). However, UTR length per se does not determine mTOR dependency because mRNAs with similarly short coding sequence (CDS) and UTR lengths, like those for cytoplasmic and mitochondrial ribosomal proteins (Supplementary Fig. 1b), were differentially sensitive to mTOR inhibition (Fig. 1g). Although it is puzzling that we find little evidence for the selective regulation of mRNAs with complex 5′ UTRs, these mRNAs may be affected, upon prolonged mTOR inhibition, by secondary consequences of the acute changes described here. Consistent with this possibility, 24–48 h of mTOR inhibition are required to exclude the cyclin D1 mRNA maximally from polysomes[15,16].

Torin 1 suppressed the translational efficiencies of all known TOP mRNAs in our data set (mean $\log_2(\Delta) = -1.49$) (Fig. 2a and Supplementary Table 2). TOP mRNAs are defined as those with a cytidine immediately after the 5′ cap, followed by an uninterrupted stretch of 4–14 pyrimidines[13,17], and tend to encode proteins associated with translation[13,18]. When averaged across known TOP mRNAs, Torin 1 depleted RF density throughout the CDS (Supplementary Fig. 2a) and shifted known TOP mRNAs (*Eef2*, *Rps20*) out of polysomes (Fig. 2e). RNA interference (RNAi)-mediated depletion of raptor, an essential mTORC1 component, also selectively inhibited the translation of TOP mRNAs (Supplementary Fig. 3).

Torin 1 also suppressed the translation of many mRNAs not previously defined as TOP mRNAs. After excluding known TOP mRNAs from analysis, we found that the ten nucleotides surrounding the predominant transcriptional start site (TSS) in the mRNAs most suppressed by mTOR inhibition were still highly enriched for pyrimidines (Fig. 2b). This enrichment could reflect the presence of previously undocumented TOP motifs and/or of similar motifs that do not meet the TOP definition. We used the database of transcriptional start sites (dbTSS)[19] as well as the RefSeq, Ensembl and University of California, Santa Cruz (UCSC) resources to examine the TSSs of the 100 mRNAs most translationally suppressed by mTOR inhibition. Fifty-seven of these were known TOP mRNAs, and, of the remaining 43, 15 had previously unrecognized TOP motifs and 13 contained a stretch of pyrimidines that was near but did not begin at the most frequent TSS. As this suggested that the established TOP motif definition might be too conservative, we defined a relaxed TOP-like motif consisting of a stretch of at least five pyrimidines within four nucleotides of the most frequent TSS. Although this motif was relatively common among all TSSs (frequency = 0.16), it was highly enriched among the most suppressed mRNAs and significantly depleted among mRNAs with a greater than average increase in translational efficiency following mTOR inhibition (Fisher's exact test P value = 3.1×10^{-8}; Supplementary Fig. 2b). Remarkably, we found that 85 of the 100 mRNAs most sensitive to mTOR inhibition are either known TOP mRNAs or contain an unrecognized TOP or TOP-like motif (Fig. 2c, d and Supplementary Table 3). Several mRNAs that failed to meet our criteria contain pyrimidine sequences interrupted by a single purine (for example, *Hspa8*), suggesting that even our TOP-like definition may be too conservative.

Like established TOP mRNAs, many previously unrecognized TOP and TOP-like mRNAs encode proteins with roles in protein synthesis (Supplementary Table 3) whereas others point to new effectors of the mTORC1 pathway (Fig. 2d). For instance, *Vim* and *Ybx1* participate in the epithelial–mesenchymal transition, a process known to be affected by mTOR inhibition[20,21]. By analysing polysome profiles prepared from Torin-1-treated cells, we confirmed that several unrecognized TOP (*Hsp90ab1*) or TOP-like mRNAs (*Vim*, *Ybx1*) were depleted from polysome fractions as strongly as established TOP mRNAs (*Rps20*, *Eef2*) (Fig. 2e). Furthermore, TOP-like and TOP motifs conferred similar degrees of mTOR-dependent translation control when placed upstream of a luciferase reporter (Supplementary Fig. 4a, b, d). Because some TOP-like mRNAs may be misannotated and actually contain canonical TOP motifs, we *in vitro* transcribed capped mRNA beginning with a single purine followed by a pyrimidine sequence and found that, like TOP mRNAs, it was translated less efficiently than an mRNA lacking this motif when mTOR was inhibited (Supplementary Fig. 4e, f). Thus, TOP and TOP-like motifs are more numerous than previously recognized and define the vast majority of mRNAs highly dependent on mTOR for translation.

How mTOR regulates TOP mRNA translation has been a persistent mystery. The S6Ks were originally considered key mediators, but later studies did not support this possibility[22,23]. Because TOP mRNA translation is less inhibited by rapamycin than dual mTOR/PI3K inhibitors and RNAi-mediated mTOR suppression[4], we suspected that it might be regulated through the 4E-BPs, which mTORC1 phosphorylates in a largely rapamycin-resistant fashion[2,24,25]. In 4E-BP1 and 4E-BP2 (also known as Eif4ebp1 and 2, respectively) double-knockout MEFs (DKO), Torin 1 had no effect on the interaction of eIF4E with eIF4G1 (Fig. 3a, b). Furthermore, in DKO cells, Torin 1 had a minimal effect on ^{35}S-Cys/Met incorporation and did not perceptibly shift ribosomes out of polysomes (Fig. 3c, d), indicating that the 4E-BPs mediate a large part of mTOR-dependent control of general translation. Moreover, ribosome profiling of vehicle- and Torin-1-treated DKO cells revealed that the distribution of Torin-1-induced changes in translational efficiency was much narrower in DKO ($\sigma = 0.225$) than in wild-type ($\sigma = 0.401$) cells (Fig. 3e), indicating that the 4E-BPs are

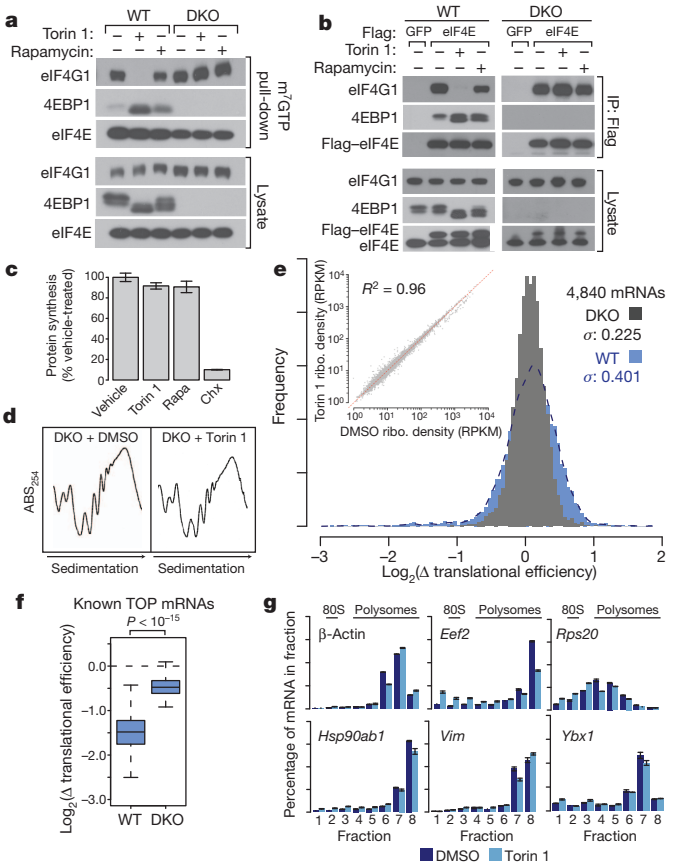

Figure 3 | mTOR regulates general protein synthesis and TOP mRNA translation through the 4E-BPs. **a**, Wild-type (WT) and 4EBP1/2 DKO MEFs were treated with DMSO, 250 nM rapamycin or Torin 1 for 2 h, lysates were subjected to m^{7}GTP pull-downs, and analysed for levels of indicated proteins. **b**, Wild-type and DKO MEFs expressing Flag–GFP or Flag–eIF4E were treated as in **a**, and immunoprecipitates (IP) analysed for indicated proteins. **c**, DKO MEFs were treated for 2 h with vehicle (DMSO), 250 nM rapamycin (Rapa) or Torin 1, or 10 μg ml^{-1} cycloheximide (Chx) were analysed as in Fig. 1b. Data are mean ± s.d. ($n = 3$). **d**, Polysome profiles of DKO MEFs treated with DMSO or Torin 1 for 2 h. **e**, Torin-1-dependent changes in translational efficiency in DKO (grey bars) and wild-type MEFs (blue bars). **f**, Torin-1-dependent translational suppression of 65 TOP mRNAs in wild-type and DKO MEFs. Significance determined by Mann–Whitney U test. **g**, Polysome analyses of selected non-TOP (β-actin), known TOP (*Eef2*, *Rps20*), unrecognized TOP (*Hsp90ab1*) and TOP-like (*Vim*, *Ybx1*) mRNAs in DKO cells. Data are means ± s.e.m. ($n = 2$).

also required for the largest translational effects caused by mTOR inhibition. Indeed, as monitored by ribosome profiling, established TOP mRNAs were barely inhibited by Torin 1 in DKO cells (Fig. 3f), which we confirmed by polysome analysis of individual mRNAs in MEFs (Fig. 3g) and in HeLa cells with RNAi-mediated knockdown of 4E-BP1 (Supplementary Fig. 5). Expression of a dominant-negative 4EBP1-4A mutant, as well as RNAi-mediated depletion of eIF4E, were sufficient to inhibit TOP mRNA translation selectively in actively growing cells (Supplementary Fig. 6). Expression of the 4EBP1-4A mutant suppressed the translation of TOP reporter constructs as well (Supplementary Fig. 4c). We found no evidence that previously identified pyrimidine-binding proteins, such as TIA1, TIAR or La (also known as SSB), have a role in the selective regulation of TOP mRNAs by mTORC1 (Supplementary Fig. 7). However, we cannot rule out a role for these proteins in the amino acid regulation of TOP mRNA translation, which is maintained in DKO cells probably through the GCN2 (also known as eIF2AK4) pathway (Supplementary Fig. 8). These results indicate that the translation of mRNAs with TOP and TOP-like motifs is highly sensitive to 4E-BP phosphorylation, and that this is the basis of their regulation by mTORC1.

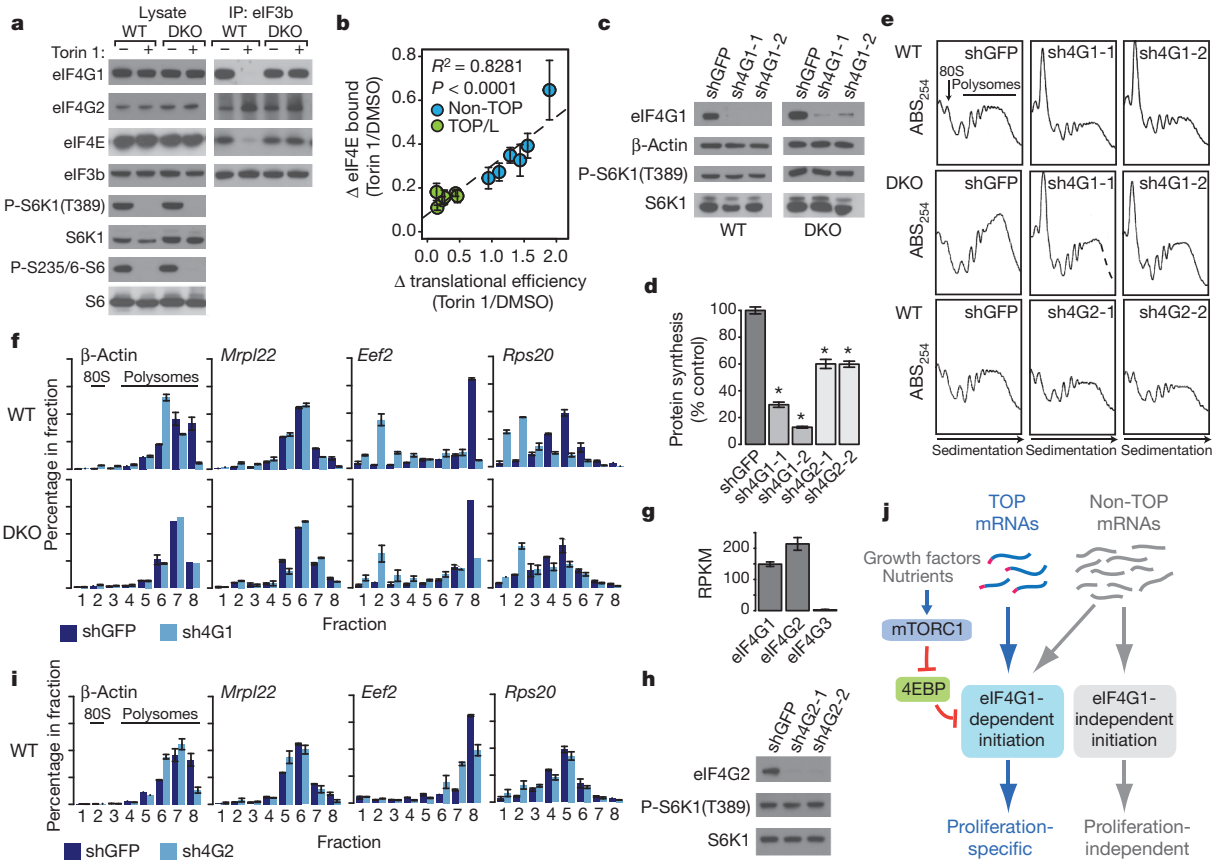

Figure 4 | Destabilization of the eIF4E–eIF4G1 interaction dissociates TOP mRNAs from eIF4E and inhibits their translation. **a**, Wild-type (WT) and DKO MEFs were treated for 2 h with DMSO or 250 nM Torin 1 and eIF3b immunoprecipitates analysed for indicated proteins. P, phospho. P-S235/236-S6 indicates S6 phosphorylated at Ser 235 and Ser 236. **b**, Flag–eIF4E was immunoprecipitated from wild-type MEFs treated with DMSO or 250 nM Torin 1 for 2 h. RNA was extracted, and the abundance of TOP and TOP-like (TOP/L) (*Eef2*, *Rps20*, *Hsp90ab1*, *Pabpc1*, *Ybx1*, *Vim*) and non-TOP (*Actb*, *Mrpl22*, *Ccnd1*, *Slc2a1*, *Gabarapl1*, *Myc*) mRNAs was quantified by qPCR. Changes in eIF4E binding of mRNAs were plotted against changes in translational efficiency from Fig. 1f. eIF4E binding data are means ± s.e.m. ($n = 4$). **c**, Levels of indicated proteins in cells expressing indicated short hairpin RNAs (shRNAs). **d**, Cells expressing indicated shRNAs were pulsed for 30 min with ^{35}S-labelled Cys/Met and analysed as in Fig. 1b. Data are means ± s.d. ($n = 3$). Significance was determined by *t*-test. *$P < 0.001$. **e**, Polysome profiles for wild-type or DKO cells expressing indicated shRNAs. **f**, RNA isolated from gradients in **e** was analysed by qPCR for the indicated mRNAs as in Fig. 1e. Data are means ± s.e.m. ($n = 2$). **g**, Abundance of indicated transcripts from RNA-Seq analysis. Data are means ± s.e.m. ($n = 3$). **h**, Lysates from cells expressing shGFP or eIF4G2-specific shRNAs were analysed by immunoblotting. **i**, Fractions from shEIF4G2-2 gradients in **e** were analysed as in **f**. **j**, mTORC1 regulates the selective translation of TOP and TOP-like mRNAs through the 4EBP-dependent control of eIF4G1-mediated initiation.

To understand why the translation of TOP and TOP-like mRNAs has a 4E-BP-mediated hyper-dependence on mTOR, we considered the established functions of the 4E-BPs[3]. A key step in eIF4E-dependent initiation is the cooperative binding of eIF4E and eIF4G1 to mRNA, which nucleates the eIF4F complex[26]. eIF4G1 also interacts with eIF3, which orchestrates assembly of the 43S pre-initiation complex on the mRNA. When mTORC1 is inactive, dephosphorylated 4E-BPs bind to eIF4E and thereby prevent its association with eIF4G1 (Fig. 3a, b). mTOR inhibition also prevents the association of eIF4G1 with eIF3 in wild-type but, unexpectedly, not in DKO cells[27] (Fig. 4a). Expression of the 4EBP1-4A mutant similarly disrupted the eIF4G1–eIF3 interaction (Supplementary Fig. 6b). Because destabilization of the eIF4F complex weakens the affinity of eIF4E for the mRNA cap[26], we hypothesized that mTOR inhibition might selectively impair the binding of eIF4E to TOP and TOP-like mRNAs. Indeed, Torin 1 treatment of cells caused a selective loss of TOP and TOP-like mRNAs from eIF4E, which strongly correlated with their degree of translational suppression (Fig. 4b). Consistent with a special role for eIF4G1 in TOP mRNA translation, RNAi-mediated depletion of eIF4G1 in wild-type cells, which mimicked the effects of Torin 1 on overall protein synthesis and polysome profiles, selectively suppressed the translation of TOP mRNAs, without affecting mTORC1 activity (Fig. 4c–f). Importantly, in the DKO cells, eIF4G1 depletion also selectively repressed TOP mRNA translation (Fig. 4c, e, f), consistent with eIF4G1 acting downstream of the 4E-BPs. A functionally redundant eIF4G1 homologue, eIF4G3, is not well expressed in the MEFs (Fig. 4g) and its loss had little effect on translation in HeLa cells (Supplementary Fig. 9). MEFs do express a distinct eIF4G1 homologue, eIF4G2 (also known as DAP5; Fig. 4g), which does not bind eIF4E but still mediates a substantial fraction of protein synthesis[28,29]. Although eIF4G2 depletion significantly suppressed overall protein synthesis, it did not have selective effects on the translation of TOP mRNAs (Fig. 4a, d, e, h, i). Therefore, unlike other mRNAs, TOP mRNAs require eIF4G1 to anchor eIF4E to the cap, and this underlies their selective translational regulation by the 4E-BPs and mTORC1.

We find that the effects of acute mTOR inhibition on mRNA translation are largely mediated by the 4E-BPs, including the moderate suppression of the translation of all mRNAs and the more marked inhibition of TOP and TOP-like mRNA translation. As the 4E-BPs are required for the mTORC1-dependent regulation of proliferation[16], the translational control of TOP mRNAs may have a fundamental role in this process (Fig. 4j), as well as in cancers associated with hyperactive mTOR signalling. We focused on suppressed mRNAs, but many other transcripts are translated with increased efficiency, and may be important for cellular survival under conditions of impaired mTORC1 signalling.

METHODS SUMMARY

To generate ribosome and mRNA profiling libraries, wild-type MEFs (*4EBP1/2*$^{+/+}$; *p53*$^{-/-}$) or DKO MEFs (4EBP1/2$^{-/-}$; *p53*$^{-/-}$) were treated with vehicle or 250 nM Torin 1 for 2 h. Cellular extracts were partitioned for either ribosome profiling or mRNA profiling. Small RNA libraries were prepared according to established protocols[8] with some modifications, and analysed by high-throughput sequencing. Transcript abundance was determined through an iterative alignment and mapping strategy to a non-redundant library of mouse transcripts based on RefSeq definitions.

Full Methods and any associated references are available in the online version of the paper at www.nature.com/nature.

Received 30 June 2011; accepted 29 March 2012.

1. Zoncu, R., Efeyan, A. & Sabatini, D. M. mTOR: from growth signal integration to cancer, diabetes and ageing. *Nature Rev. Mol. Cell Biol.* **12,** 21–35 (2011).
2. Thoreen, C. C. *et al.* An ATP-competitive mammalian target of rapamycin inhibitor reveals rapamycin-resistant functions of mTORC1. *J. Biol. Chem.* **284,** 8023–8032 (2009).
3. Hay, N. & Sonenberg, N. Upstream and downstream of mTOR. *Genes Dev.* **18,** 1926–1945 (2004).
4. Patursky-Polischuk, I. *et al.* The TSC-mTOR pathway mediates translational activation of TOP mRNAs by insulin largely in a raptor- or rictor-independent manner. *Mol. Cell. Biol.* **29,** 640–649 (2009).
5. Bilanges, B. *et al.* Tuberous sclerosis complex proteins 1 and 2 control serum-dependent translation in a TOP-dependent and -independent manner. *Mol. Cell. Biol.* **27,** 5746–5764 (2007).
6. Gera, J. F. *et al.* AKT activity determines sensitivity to mammalian target of rapamycin (mTOR) inhibitors by regulating cyclin D1 and c-*myc* expression. *J. Biol. Chem.* **279,** 2737–2746 (2004).
7. Grolleau, A. *et al.* Global and specific translational control by rapamycin in T cells uncovered by microarrays and proteomics. *J. Biol. Chem.* **277,** 22175–22184 (2002).
8. Ingolia, N. T., Ghaemmaghami, S., Newman, J. R. & Weissman, J. S. Genome-wide analysis *in vivo* of translation with nucleotide resolution using ribosome profiling. *Science* **324,** 218–223 (2009).
9. Redman, K. L. & Rechsteiner, M. Identification of the long ubiquitin extension as ribosomal protein S27a. *Nature* **338,** 438–440 (1989).
10. Mokrejs, M. *et al.* IRESite—a tool for the examination of viral and cellular internal ribosome entry sites. *Nucleic Acids Res.* **38,** D131–D136 (2010).
11. Kozak, M. A second look at cellular mRNA sequences said to function as internal ribosome entry sites. *Nucleic Acids Res.* **33,** 6593–6602 (2005).
12. Martin, F. *et al.* Cap-assisted internal initiation of translation of histone H4. *Mol. Cell* **41,** 197–209 (2011).
13. Meyuhas, O. Synthesis of the translational apparatus is regulated at the translational level. *Eur. J. Biochem.* **267,** 6321–6330 (2000).
14. De Benedetti, A. & Graff, J. R. eIF-4E expression and its role in malignancies and metastases. *Oncogene* **23,** 3189–3199 (2004).
15. Shi, Y., Sharma, A., Wu, H., Lichtenstein, A. & Gera, J. Cyclin D1 and c-*myc* internal ribosome entry site (IRES)-dependent translation is regulated by AKT activity and enhanced by rapamycin through a p38 MAPK- and ERK-dependent pathway. *J. Biol. Chem.* **280,** 10964–10973 (2005).
16. Dowling, R. J. *et al.* mTORC1-mediated cell proliferation, but not cell growth, controlled by the 4E-BPs. *Science* **328,** 1172–1176 (2010).
17. Jefferies, H. B., Reinhard, C., Kozma, S. C. & Thomas, G. Rapamycin selectively represses translation of the "polypyrimidine tract" mRNA family. *Proc. Natl Acad. Sci. USA* **91,** 4441–4445 (1994).
18. Iadevaia, V., Caldarola, S., Tino, E., Amaldi, F. & Loreni, F. All translation elongation factors and the e, f, and h subunits of translation initiation factor 3 are encoded by 5′-terminal oligopyrimidine (TOP) mRNAs. *RNA* **14,** 1730–1736 (2008).
19. Yamashita, R., Wakaguri, H., Sugano, S., Suzuki, Y. & Nakai, K. DBTSS provides a tissue specific dynamic view of transcription start sites. *Nucleic Acids Res.* **38,** D98–D104 (2010).
20. Lamouille, S. & Derynck, R. Cell size and invasion in TGF-β-induced epithelial to mesenchymal transition is regulated by activation of the mTOR pathway. *J. Cell Biol.* **178,** 437–451 (2007).
21. Thiery, J. P., Acloque, H., Huang, R. Y. & Nieto, M. A. Epithelial-mesenchymal transitions in development and disease. *Cell* **139,** 871–890 (2009).
22. Jefferies, H. B. *et al.* Rapamycin suppresses 5′TOP mRNA translation through inhibition of p70s6k. *EMBO J.* **16,** 3693–3704 (1997).
23. Pende, M. *et al. S6K1*$^{-/-}$/*S6K2*$^{-/-}$ mice exhibit perinatal lethality and rapamycin-sensitive 5′-terminal oligopyrimidine mRNA translation and reveal a mitogen-activated protein kinase-dependent S6 kinase pathway. *Mol. Cell. Biol.* **24,** 3112–3124 (2004).
24. Choo, A. Y., Yoon, S. O., Kim, S. G., Roux, P. P. & Blenis, J. Rapamycin differentially inhibits S6Ks and 4E-BP1 to mediate cell-type-specific repression of mRNA translation. *Proc. Natl Acad. Sci. USA* **105,** 17414–17419 (2008).
25. Feldman, M. E. *et al.* Active-site inhibitors of mTOR target rapamycin-resistant outputs of mTORC1 and mTORC2. *PLoS Biol.* **7,** e38 (2009).
26. Ptushkina, M. *et al.* Cooperative modulation by eIF4G of eIF4E-binding to the mRNA 5′ cap in yeast involves a site partially shared by p20. *EMBO J.* **17,** 4798–4808 (1998).
27. Harris, T. E. *et al.* mTOR-dependent stimulation of the association of eIF4G and eIF3 by insulin. *EMBO J* **25,** 1659–1668 (2006).
28. Lee, S. H. & McCormick, F. p97/DAP5 is a ribosome-associated factor that facilitates protein synthesis and cell proliferation by modulating the synthesis of cell cycle proteins. *EMBO J.* **25,** 4008–4019 (2006).
29. Ramirez-Valle, F., Braunstein, S., Zavadil, J., Formenti, S. C. & Schneider, R. J. eIF4GI links nutrient sensing by mTOR to cell proliferation and inhibition of autophagy. *J. Cell Biol.* **181,** 293–307 (2008).

Supplementary Information is linked to the online version of the paper at www.nature.com/nature.

Acknowledgements We thank members of the Gray and Sabatini laboratories for helpful discussions, H. Guo, S. Hawthorne, G. Brar, J. Damon, C. Miller and W. Gilbert for advice and N. Sonenberg for providing 4EBP1/2 wild-type and double-knockout MEFs. This work was supported by the National Institutes of Health (CA103866 and CA129105 to D.M.S.), Department of Defense (W81XWH-07-0448 to D.M.S.), the W.M. Keck Foundation (D.M.S.), LAM Foundation (D.M.S.), Dana Farber Cancer Institute (N.S.G., C.C.T.), and fellowship support from the American Cancer Society (C.C.T.), and the National Science Foundation (L.C. and T.W.). D.M.S. is an investigator of the Howard Hughes Medical Institute.

Author Contributions C.C.T. and D.M.S. conceived the project. C.C.T. designed and performed most experiments and data analyses with input from D.M.S. and N.S.G. L.C. and H.R.K. assisted with experiments and T.W. with sequence analysis. C.C.T. and D.M.S. wrote and edited the manuscript with input from N.S.G.

Author Information Small RNA sequencing data were deposited in the Gene Expression Omnibus (http://www.ncbi.nlm.nih.gov/geo) under accession number GSE36892. Reprints and permissions information is available at www.nature.com/reprints. The authors declare no competing financial interests. Readers are welcome to comment on the online version of this article at www.nature.com/nature. Correspondence and requests for materials should be addressed to N.S.G. (nathanael_gray@dfci.harvard.edu) or D.M.S. (sabatini@wi.mit.edu).

METHODS

Materials. Reagents were obtained from the following sources: antibodies to phospho-Thr-389 S6K, S6, 4EBP1, eIF4E, phospho-S51 eIF2α, eIF2α, eIF4G1 and eIF4G2 from Cell Signaling; antibodies to eIF3b (N20), β-actin, S6K and horseradish-peroxidase-labelled anti-mouse, anti-goat and anti-rabbit secondary antibodies from Santa Cruz Biotechnology; FuGENE 6 and Complete Protease Mixture from Roche Applied Science; Flag M2-agarose and cycloheximide from Sigma; 7-methyl-GTP-Sepharose from GE Healthcare; rapamycin from LC Laboratories; luciferase mRNA and luciferase assay reagents from Promega; EasyTagTM EXPRESS ^{35}S protein labelling mix from PerkinElmer Life Sciences; acid phenol/chloroform/isoamyl alcohol, GlycoBlue, SuperaseIn and Proteinase K from Ambion. Polynucleotide kinase (PNK), polyA polymerase, Phusion High Fidelity DNA polymerase, and RNase I_f, T7 RNA polymerase, DNase I and m7GpppG cap analogue from New England Biolabs; Circligase from Epicentre Biotechnologies; Ecl136 from Fermentas; DMEM from SAFC Biosciences; TransMessenger transfection reagent from Qiagen; inactivated fetal calf serum and oligo dT_{25} Dynabeads from Invitrogen. *4EBP1/2*$^{+/+}$; *p53*$^{-/-}$ MEFs and *4EBP1/2*$^{-/-}$; *p53*$^{-/-}$ MEFs were provided by N. Sonenberg (McGill University). Torin 1 was synthesized and purified in the Gray laboratory[30] and is commercially available from Tocris.

Preparation of cell lysates and affinity purifications. Cells were rinsed once with ice-cold PBS and lysed in ice-cold lysis buffer (buffer A: 50 mM HEPES-KOH (pH 7.4), 2 mM EDTA, 10 mM pyrophosphate, 10 mM β-glycerophosphate, 40 mM NaCl, 1% Trition X-100 and one tablet of EDTA-free protease inhibitors (Roche) per 25 ml). The soluble fractions of cell lysates were isolated by centrifugation at 13,000*g* for 10 min. For immunoprecipitations, primary antibodies were added to lysates and incubated with rotation for 2 h at 4 °C. 20 µl of a 50% slurry of protein G-sepharose was then added and the incubation continued for an additional 1 h. Immunoprecipitates were washed three times with lysis buffer. Immunoprecipitated proteins were denatured by the addition of 20 µl of sample buffer and boiling for 5 min, resolved by 8–16% SDS–PAGE, and analysed by western blot. For Flag purifications, Flag M2 affinity gel was washed with lysis buffer three times. 20 µl of beads in 50% slurry was then added to cell lysates and incubated with rotation for 2 h at 4 °C. Finally, beads were washed three times with lysis buffer. Immunoprecipitated proteins were denatured by the addition of 50 µl of sample buffer and boiling for 5 min. For m7GTP affinity purifications, m7GTP sepharose was washed with lysis buffer. 20 µl of beads in 50% slurry was added to cell lysates and incubated with rotation for 2 h at 4 °C. Finally, beads were washed three times with lysis buffer, denatured by the addition of 50 µl sample buffer and analysed by western blot. For amino acid starvation, cells were washed twice in amino acid-free RPMI and then incubated in RPMI containing 10% dialysed FBS with or without amino acids.

Metabolic labelling of cells. Cells were seeded in 6-well plates and cultured overnight. Cells were then treated with appropriate compounds for 2 h, washed once with cysteine/methionine-free DMEM, and then incubated in 2 ml of cysteine/methionine-free DMEM, 10% dialysed inactivated fetal calf serum, compound, and 165 µCi (15 µl, 11 µCi µl^{-1}) of EasyTag EXPRESS ^{35}S protein labelling mix. After 30 min, cells were lysed, and soluble fractions were isolated by centrifugation at 13,000*g* for 10 min. Lysates were then spotted on Whatman filter paper and protein was precipitated with 5% trichloroacetic acid, washed two times for 5 min in cold 10% trichloroacetic acid, washed two times for 2 min in cold ethanol, washed one time for 2 min in acetone, and air-dried at room temperature (25 °C). The amount of ^{35}S incorporated into protein was measured using a Beckman LS6500 Scintillation Counter. Total protein content was determined by Bradford assay (Bio-rad).

Mammalian lentiviral shRNAs and cDNAs. All shRNA vectors were obtained from the collection of The RNAi Consortium at the Broad Institute[31]. These shRNAs are named with the numbers found at the RNAi Consortium public website: mouse *shEif4g1-1* (TRCN0000096809), mouse *shEif4g1-2* (TRCN0000096811), mouse *shEif4g2-1* (TRCN0000009807), mouse *shEif4g2-2* (TRCN0000009809), mouse *shEif4e-1* (TRCN0000077475), mouse *shEif4e-2* (TRCN0000077477), mouse *shTia1* (TRCN0000077161), mouse *shTiar* (TRCN0000102619), mouse shRaptor (TRCN0000077472), human *sh4EBP1* (TRCN0000040203), human *sh4EBP2* (TRCN0000117814), human *shEIF4G1-1* (TRCN0000061769), human *shEIF4G1-2* (TRCN0000061770), human *shEIF4G3-1* (TRCN0000142702), human *shEIF4G3-2* (TRCN0000139543). shRNA-encoding plasmids were co-transfected with the psPax2 envelope and vesicular stomatitis virus G packaging plasmids into actively growing HEK-293T using FuGENE 6 transfection reagent as described previously[32]. Virus-containing supernatants were collected at 48 h after transfection and filtered to eliminate cells, and target cells were infected in the presence of 8 µg ml^{-1} polybrene. Twenty-four hours later, cells were selected with puromycin and analysed on the fourth day after infection. 4EBP1-4A mutant was constructed by mutating T36, T47, S65 and T70 residues of rat 4EBP1 to alanines, which was then inserted into a Tet-On plasmid.

Polysome analysis, RNA isolation, and qPCR. Cells were seeded in 15 cm dishes at 5×10^6 cells per dish and cultured overnight. Cells were then treated with 100 µg ml^{-1} cycloheximide for 5 min before lysis, washed in ice-cold PBS− (PBS lacking calcium) plus 100 µg ml^{-1} cycloheximide, and then lysed in polysome lysis buffer (15 mM HEPES-KOH (pH 7.4), 7.5 mM $MgCl_2$, 100 mM KCl, 2 mM DTT, 1.0% Triton X-100, 100 µg ml^{-1} cycloheximide, and one tablet of EDTA-free protease inhibitors (Roche) per 25 ml). Lysates were normalized by protein content using Bradford reagent (Bio-rad) and either layered onto 11 ml 10–50% sucrose density gradients (15 mM HEPES-KOH, 7.5 mM $MgCl_2$, 100 mM KCl, 2 mM DTT, 100 µg ml^{-1} cycloheximide, 20 U ml^{-1} SuperaseIn, 10–50% RNase-free sucrose) or adjusted to 0.5% SDS and reserved for total RNA isolation. Gradients were centrifuged in an SW-41Ti rotor at 32,000 r.p.m. at 4 °C for 2 h, and then sampled using a Labconco Auto Densi-Flow Gradient Fractionator connected to an Isco Tris pump with constant monitoring of optical density (OD) at 254 nM. 1 ml fractions were collected throughout, adjusted to 0.5% SDS and incubated at 65 °C for 5 min. 5 ng of polyA+ synthetic luciferase mRNA (Promega) was added to each fraction for normalization. Samples were then treated with 200 µg ml^{-1} Proteinase K (Ambion) and digested for 45 min at 50 °C, followed by 1:1 dilution with RNase-free water. RNA was extracted from diluted fractions using the hot acid phenol method, and precipitated with NaOAc and isopropanol. cDNA was prepared using the Superscript III reverse transcriptase (Invitrogen) with random hexamer primers according to the manufacturer's instructions. Transcript abundance was determined by quantitative PCR (qPCR) using SYBR Green PCR mix (Applied Biosystems) and primers specific for each transcript. Measurements were then normalized to luciferase abundance, and plotted as per cent detected.

Oligonucleotides used for qPCR of mouse mRNAs are as follows. *Eef2*: forward 5′-GAGAATCCGTCGCCATCCGCCA-3′, reverse 5′-CGGGCTTGATGCGTTCAGCGA-3′; β-actin: forward 5′-TCGTTGCCGGTCCACACCCG-3′, reverse 5′-CTCCTCAGGGGCCACACGCAG-3′; *Mrpl22*: forward 5′-TCTGGGCAACGCAGACGCTG-3′, reverse 5′-GCCAAAGCGACCTCGGCCAT-3′; *Rps20*: forward 5′-TGACTCACCGCTGTTCGCTCC-3′, reverse 5′-GAGTCGCTTGTGGATCCTCATCTGG-3′; *Hsp90ab1*: forward 5′-GCCGTGCGAGTCGGACTTGGT-3′, reverse 5′-CCGACACCAAACTGCCCGATCA-3′; *Vim*: forward 5′-ACTGCTGCCCTGCGTGATGT-3′, reverse 5′-TCTCACGCATCTGGCGCTCC-3′; *Ybx1*: forward 5′-GGGGTCCTCCACGCAATTACC-3′, reverse 5′-CGGCGATACCGACGTTGAGGT-3′; *Pabpc1*: 5′-CGCTGGACTGCTCAGGGTGC-3′, reverse 5′-GGGGGCGCAGATGCCAACAT-3′; *Myc*: forward 5′-GCCAGCCCTGAGCCCCTAGT-3′, reverse 5′-GGGTGCGGCGTAGTTGTGCT-3′; *Gabarapl1*: 5′-AGCCCCCAAAGCTCGGATAGGA-3′, reverse 5′-GGTGTTCCTGGTACAGCTGACCC-3′; *Slc2a1*: forward 5′-CTGGCATGGCAGGCTGTGCT-3′, reverse 5′-CGCCCCCAGAGGGTGGAAGA-3′; *Ccnd1*: forward 5′-GCCCGAGGAGCTGCTGCAAA-3′, reverse 5′-GCCTTGCATCGCAGCCACCA-3′; firefly luciferase: forward 5′-ATCCGGAAGCGACCAACGCC-3′, reverse 5′-GTCGGGAAGACCTGCCACGC-3′.

Oligonucleotides used for qPCR of human mRNAs are as follows. β-Actin: forward 5′-AGCCTCGCCTTTGCCGA-3′, reverse 5′-GCGCGGCGATATCATCATC-3′; *Gnb2l*: forward 5′-TGGGATCTCACAACGGGCACCA-3′, reverse 5′-CCGGTTGTCAGAGGAGAAGGCCA-3′; *Rps20*: forward 5′-CCAGTTCGAATGCCTACCAAGACTT-3′, reverse 5′-ACTTCCACCTCAACTCCTGGCTCA-3′; *eIF4G3*: forward 5′-CCAGAGGGCCTGCCTCCTATCA-3′, reverse 5′-TGGCAATCCATGCCTGCTCTGC-3′.

Protein–RNA co-immunoprecipitation assays. MEFs stably expressing the indicated Flag-tagged constructs were seeded in 10 cm plates at 2×10^6 cells per plate and incubated overnight. Cells were then treated with vehicle or 250 nM Torin 1 for 2 h, and lysed in buffer A (see earlier) containing 40 U ml^{-1} SuperaseIn. Insoluble material was removed by centrifugation and lysates were normalized by protein concentration and incubated with Flag-M2 agarose for 2 h at 4 °C with rotation. Immunoprecipitates were then washed six times with 1 ml buffer A, twice with polysome lysis buffer, and eluted with 100 µl 3×Flag peptide in polysome lysis buffer for 10 min at 37 °C. Eluates were divided into portions for immunoblotting and RNA extraction. For RNA extractions, 10 ng luciferase mRNA, 1 µg yeast tRNA, 200 µg ml^{-1} proteinase K and SDS (0.5% final concentration) were added to eluates, which were then incubated at 50 °C for 45 min. RNA was extracted twice with acid phenol, once with chloroform and precipitated with NaOAc and isopropanol. Isolated RNA was used as a template for cDNA synthesis using oligo-dT primers, and analysed by qPCR. mRNA abundance in each sample was normalized to spike-in luciferase. For western blotting, sample buffer was added to eluates, which were analysed as described earlier.

Luciferase reporter assays. For luciferase reporter assays, plasmids were constructed by cloning the 5′ UTRs and 1 kb of upstream sequence into a derivative

of the pIS1 renilla luciferase expression vector where the CMV promoter had been excised. The pIS1 3′ UTR was maintained intact. The *Vim*/*Actb* hybrid 5′ UTR reporter was constructed by replacing the promoter and first 30 nucleotides of the *Actb* reporter with the promoter and first 30 nucleotides of the *Vim* reporter. Cells were then seeded in 6-well plates at 10^5 cells per well and simultaneously transfected with 100 ng of the indicated reporter plasmid and 400 ng of empty vector. After an overnight incubation, cells were washed with fresh media and treated with either vehicle or 250 nM Torin 1 for 24 h. Luciferase expression was quantified using the Renilla Luciferase Assay System (Promega) according to the manufacturer's directions using a standard laboratory luminometer.

For mRNA transfection experiments, *Eef2* and *Actb* 5′ UTRs immediately preceded by a T7 RNA polymerase promoter were cloned into a derivative of pRL containing a renilla luciferase open reading frame (ORF), a short 3′ UTR and poly(A)$_{62}$ tail followed by an Ecl136 restriction site. 50 μg of each reporter plasmid were digested overnight with Ecl136, purified by phenol-chloroform extraction, and used as a template for T7 RNA polymerase in reactions containing a fivefold excess of m7GpppG cap analogue. mRNA was then purified by acid phenol extraction. For transfection, cells were seeded in 24-well plates at 50,000 cells per well and transfected with 200 ng *Eef2* or *Actb* renilla luciferase reporter mRNA and 200 ng of a control firefly luciferase mRNA for 2 h using the TransMessenger mRNA transfection reagent according to the manufacturer's directions. Cells were then washed with fresh media containing serum, incubated for 1 h, and then treated with vehicle or 250 nM Torin 1. After a 16 h incubation, luciferase production was quantified using the Dual Luciferase Reporter Assay (Promega) according to the manufacturer's directions. Renilla expression values were then normalized to firefly expression values to control for transfection efficiency.

Small RNA library preparation. Footprint libraries were prepared as described previously with minor modifications[8]. Briefly, cells were seeded in 15 cm dishes at 5×10^6 cells per plate and cultured overnight. Importantly, we ensured that cells had not reached confluency by the following day, as confluency is known to significantly affect mRNA translation[33]. Cells were then treated with vehicle (DMSO), rapamycin or Torin 1 for 2 h. Five minutes before lysis, 100 μg ml^{-1} cycloheximide was added to each plate. Cells were then washed once with ice-cold PBS− plus 100 μg ml^{-1} cycloheximide, and lysed in footprint lysis buffer (15 mM HEPES-KOH (pH 7.4), 7.5 mM $MgCl_2$, 300 mM KCl, 100 μg ml^{-1} cycloheximide, 2 mM DTT, 1.0% Triton X-100, 1 tablet of EDTA-free protease inhibitors (Roche) per 25 ml). Lysates were cleared by centrifugation at 13,000*g* at 4 °C for 10 min, and supernatants were transferred to clean tubes. RNase I_f was added to a final concentration of 1 U μl^{-1}, and samples were incubated at 25 °C for 45 min with constant rotation. Digested samples were then layered onto 10–50% sucrose density gradients (15 mM HEPES-KOH (pH 7.4), 7.5 mM $MgCl_2$, 300 mM KCl, 2 mM DTT, 100 μg ml^{-1} cycloheximide, 20 U ml^{-1} SuperaseIn, 10–50% RNase-free sucrose) and centrifuged in an SW-41Ti rotor at 36,000 r.p.m. for 2.5 h. Gradients were fractionated as described for polysome analysis, and monosome fractions were collected and reserved. Samples were adjusted to 0.5% SDS and digested with 200 μg ml^{-1} proteinase K at 50 °C for 45 min. RNA was extracted using the hot acid phenol method, and precipitated with NaOAc and isopropanol. RNA was next resuspended in 500 μl 10 mM Tris 8 plus 2.5 μl SuperaseIn and centrifuged for 28 min in a Millipore YM100 micro-concentrator to remove RNA fragments longer than 100 nucleotides. RNA was preciptated from flow-through and separated on a 15% TBE-Urea gel, which revealed a clear band at ~30 nucleotides. RNA was extracted from this region of the gel and quantified using an Agilent BioAnaylzer. Samples were normalized to equivalent concentrations, and prepared for small RNA Illumina sequencing precisely as previously described[8].

For total mRNA isolation, vehicle- or Torin-1-treated cells were washed in ice-cold PBS− and lysed in total RNA lysis buffer (15 mM HEPES-KOH (pH 7.4), 15 mM $MgCl_2$, 0.3 M NaCl, 1.0% SDS). Lysates were homogenized by serial passage through a 21G needle and incubated at 65 °C for 5 min. RNA was then extracted using the hot acid phenol method and re-suspended in 200 μl 10 mM Tris 8. PolyA+ RNA was isolated from 150 μg total RNA using oligo dT_{25} Dynabeads (Invitrogen) according to the manufacturer's instructions, resuspended in 20 μl 10 mM Tris 8, and then fragmented by the addition of 20 μl fragmentation buffer (2 mM EDTA, 100 mM $NaCO_3$ pH 9.2) and incubation at 95 °C for 20 min. Fragmented RNA was precipitated and separated on a 15% TBE-Urea gel. Short RNA fragments were then isolated from the 30-nucleotide region and quantified using an Agilent Bioanalyzer. Samples were normalized to equal concentrations and prepared for Illumina small RNA sequencing in parallel with footprint samples. Footprint libraries were prepared in two biological replicates, whereas total transcript libraries were prepared as single replicates.

RNA sequence analyses. Before alignment, footprint and total mRNA libraries were processed to remove cloning artefacts. Processed reads were then aligned to a database of mouse rRNA sequences using the Bowtie short-read alignment program to remove contaminating reads[34]. These rRNA reads represented 40–80% of the footprint libraries, consistent with previous work[8,35]. The remaining reads were then aligned to the mm9 mouse genome. Reads that failed to align to genomic positions were re-aligned to a database of RefSeq gene sequences to capture those mapping to splice junctions. For both alignments, two mismatches were allowed in a 25-nucleotide 'seed' region, and reads were required to align to a single unique location. The resulting aligned libraries were then mapped to gene models described by the RefSeq annotation, which was downloaded from the UCSC genome browser website in March, 2010. Reads mapping to a unique genomic location, but to multiple transcripts, were counted equally for each transcript. Many mammalian genes have duplicate pseudogenes that exist throughout the genome, thereby causing reads that map to those genes to be discarded because they fail to map to a single unique location. To avoid under-counting these genes, the alignment process was repeated for previously unaligned reads using the same parameters, but allowing alignment at up to five unique sites. Counts for these 'multi-reads' were then distributed to each mapped gene model according to their relative representation in our library of unique alignments, similar to a strategy described previously[36]. Expression values were calculated as a modified version of RPKM, which normalizes mapped reads to gene length and library size[36]. The original RPKM value is calculated as $R_i = 10^9(C_i/NL_i)$, where C_i is the number of reads mapped to exons of gene i, N is the number of mapped reads in the entire library, and L_i is the length of the spliced gene in nucleotides. Because contaminating rRNA constitutes a large part of our sequenced library, we calculated N as the number of reads mapping to exons of coding gene models. Translational efficiency was calculated as footprint (RPKM)/mRNA (RPKM). Values from biological replicates were averaged together.

Several additional constraints were applied before calculating changes in translational efficiency between vehicle- and Torin-1-treated conditions. First, we considered only genes where the combined number of reads between vehicle- and Torin-1-treated conditions exceeded 128. As reported previously, the replicate error in fold-change calculations for genes with fewer reads is primarily due to simple binomial sampling error[8]. Second, we considered only transcripts encoding protein-coding genes, and further excluded a small number of transcripts where greater than 25% of footprint reads mapped to introns. Three pseudogenes with homology to ribosomal protein coding genes were removed manually (NM_001081036 and NM_001111116, NM_001101561). Last, we calculated translational changes for histone mRNAs from footprint reads only. Histone mRNAs were present in footprint libraries, but, because they have no polyA tail, could not be reliably detected in total mRNA libraries.

Analysis of footprint libraries can be used to determine the proportion of ribosomes engaged in translating each mRNA within each sample (RPM, reads per million), but can't directly measure differences in the overall number of translating ribosomes between samples. However, measurements of ^{35}S Cys/Met incorporation show that mTOR inhibition reduces the overall rate of protein synthesis by ~65%. Because mTOR primarily regulates initiation steps in translation, and because polysome analysis of Torin-1-treated cells clearly demonstrates a severe defect in initiation, the reduction in ^{35}S Cys/Met incorporation predominantly reflects a reduction in the number of translating ribosomes. Therefore, an mRNA that is translated by the same proportion of ribosomes in vehicle- and Torin-1-treated conditions is translated by approximately 65% fewer ribosomes when mTOR is inhibited. This factor can be incorporated as $\Delta_{\text{translation}} = \Delta_{\text{ribosome density}} \times \Delta_{\text{translating ribosomes}}$ for each mRNA, where $\Delta_{\text{ribosome density}}$ is the change in footprint RPM and $\Delta_{\text{translating ribosomes}} = 0.35$ (65% reduction). Applying this correction, we find that all but four mRNAs are translated by fewer ribosomes in Torin-1-treated cells than in vehicle-treated cells.

Complexity of 5′ UTRs. The 5′ UTR sequences all of transcripts were obtained from the NCBI Reference Sequence collection. The minimum folding ΔG° were predicted for each sequence using QuikFold2 (http://mfold.rna.albany.edu/?q=DINAMelt/Quickfold) with the default parameters for version 3.0 of the RNA folding energy rules[37].

Gene ontology and TOP-like analysis. To determine enrichment for gene ontology categories, mRNAs with a z-score greater than 1.5 or less than −1.5 were analysed using the Database for Annotation, Visualization, and Integrated Discovery (DAVID) website (http://david.abcc.ncifcrf.gov/)[38,39]. The 4,840 protein-coding mRNAs that were detected in both wild-type and DKO cells were used as a background reference set. Functional categories were clustered using the Functional Annotation Clustering tool, and representative gene ontology categories from each clustered set with a P value < 0.05 and FDR $< 25\%$ were selected.

For determination of TOP-like motifs, TSSs were first identified according to the experimentally determined database of TSSs from mouse NIH3T3 cells (dbTSS)[19]. For each mRNA, only promoters with a TSS tag of parts per million (p.p.m.) > 5 were considered. An mRNA was determined as TOP if the first nucleotide was a C followed by at least four pyrimidines, and TOP-like if it

contained a sequence of at least five pyrimidines within four nucleotides of either the most frequently detected TSS or a clear secondary TSS with a TSS-tag count of at least 30% of the primary site. Because dbTSS does not have confident TSS determinations for all mRNAs, and because data are from a single mouse cell line (3T3), we also considered TSS annotations from RefSeq, Ensembl or UCSC resources (downloaded from the UCSC genome browser May, 2011).

30. Liu, Q. *et al.* Discovery of 1-(4-(4-propionylpiperazin-1-yl)-3-(trifluoromethyl)phenyl)-9-(quinolin-3- yl)benzo[h][1,6]naphthyridin-2(1*H*)-one as a highly potent, selective mammalian target of rapamycin (mTOR) inhibitor for the treatment of cancer. *J. Med. Chem.* **53,** 7146–7155 (2010).
31. Moffat, J. *et al.* A lentiviral RNAi library for human and mouse genes applied to an arrayed viral high-content screen. *Cell* **124,** 1283–1298 (2006).
32. Ali, S. M. & Sabatini, D. M. Structure of S6 kinase 1 determines whether raptor-mTOR or rictor-mTOR phosphorylates its hydrophobic motif site. *J. Biol. Chem.* **280,** 19445–19448 (2005).
33. Levine, E. M., Becker, Y., Boone, C. W. & Eagle, H. Contact inhibition, macromolecular synthesis, and polyribosomes in cultured human diploid fibroblasts. *Proc. Natl Acad. Sci. USA* **53,** 350–356 (1965).
34. Langmead, B. Aligning short sequencing reads with Bowtie. *Curr. Protoc. Bioinformatics* Chapter 11, Unit 11.7 (2010).
35. Guo, H., Ingolia, N. T., Weissman, J. S. & Bartel, D. P. Mammalian microRNAs predominantly act to decrease target mRNA levels. *Nature* **466,** 835–840 (2010).
36. Mortazavi, A., Williams, B. A., McCue, K., Schaeffer, L. & Wold, B. Mapping and quantifying mammalian transcriptomes by RNA-Seq. *Nature Methods* **5,** 621–628 (2008).
37. Markham, N. R. & Zuker, M. DINAMelt web server for nucleic acid melting prediction. *Nucleic Acids Res.* **33,** W577–W581 (2005).
38. Huang, D. WSherman, B. TLempicki, R. A. Systematic and integrative analysis of large gene lists using DAVID bioinformatics resources. *Nature Protocols* **4,** 44–57 (2009).
39. Huang, D. W. Sherman, B. T. & Lempicki, R. A. Bioinformatics enrichment tools: paths toward the comprehensive functional analysis of large gene lists. *Nucleic Acids Res.* **37,** 1–13 (2009).